

Analysis of the Impact Behavior for Different Configurations of an Experimental 30×165 mm AP-T Projectile

Alexandru SAVASTRE, Cătălin FRĂȚILĂ, Irina CÂRCEANU, and Adrian BOLOJAN

Abstract— The present study is based on numerical simulation of impact for three different nose shape 30mm AP-T Naval projectiles on a steel plate. Rigid hardened projectiles of three different geometries (Blunt, Truncated Cone and Hollow Point) keeping the same caliber were used. These projectiles were impacted on square AISI 4340 steel plates at a velocity of 890m/s without lightweight ballistic cape. The perforation capabilities were observed and the residual velocities were measured after perforation. Numerical simulations were performed in ANSYS Explicit Dynamics finite element analyze code, with the main purpose of choosing the best geometrical shape for an armor piercing projectile.

IndexTerms—AP-T, projectile, naval gun, ballistic simulation, numerical simulation.

I. INTRODUCTION

The 30x165mm AP-T ammunition analyzed in this paper is designed for use by naval CIWS (close-in weapon system) AK-630 or AK-306.

An armor-piercing projectile (AP for short), is a type of ammunition designed to penetrate armor. They were first introduced to troops during World War I, when armored vehicles appeared on the battlefield. In ship and coastal artillery, armor-piercing projectiles have always been the basis of the fire unit of ships and coastal mounted artillery. The major application of naval armor-piercing projectiles was to defeat the thick armor carried on many warships and cause damage to the lightly-armored interior. Nowadays, this type of ammunition is also suitable against aircrafts, missiles and small pirate boats.

Armor-piercing projectiles are generally cast from a special mixture of chrome steel melted and forged into shape. The shell is then thoroughly annealed, the core bored and the exterior turned up in the lathe. The shell is finished in a similar manner to others described below. The final or tempering treatment is very important, but details are kept strictly secret. It consists in hardening the head of the projectile and tempering it in a special manner, the rear portion being reduced in hardness so as to render it tough [1].

This work was supported by a grant of the Romanian Ministry of Education and Research, CCCDI – UEFISCDI, project number PN-III-P2-2.1-PTE-2019-0316, within PNCDI III.

A. SAVASTRE is with the Research Center for Navy, Constanta, Romania (e-mail: alexandru.savastre@navy.ro).

C. FRĂȚILĂ is with the Research Center for Navy, Constanta, Romania (e-mail: catalin.fratila@navy.ro).

I. CÂRCEANU is with the ROMARM National Company, Bucharest, Romania (e-mail: irina_carceanu@yahoo.co.uk).

A. BOLOJAN is with the ROMARM National Company, 061301, Bucharest, Romania (e-mail: consilier3@romarm.ro).

A primary condition for armor-piercing projectiles is that the kinetic energy should be as high as possible when is hitting the obstacle. This energy depends on the mass and velocity of the projectile at the time of impact with the armor [2].

During the penetration of the projectile into the obstacle, on its body acts the resistance force of the obstacle and the moment of this force, which tend to reduce to zero the velocity of the projectile. As a result of this action, strong forces of inertia appear in the body of the projectile. When hitting the obstacle and during its perforation, local deformations and even destruction of the projectile body are allowed. Cracks that do not penetrate deep into the body of the projectile, the tearing of the surface layers of metal, the detachment of the ogival part and the twisting or distortion of the body are admissible deformations of the projectile on impact with the obstacle [3].

Of course, the existence of such deformations leads to the consumption of some of the projectile's remaining kinetic energy and to the reduction of the penetration effect. In order to perform the maximum mechanical work on the obstacle, it is desirable that the projectiles deformations to be minimal during the perforation of the obstacle.

The projectile geometry with the nose shape is an important factor affecting the mechanism of deformation of the target plates and relatively fewer studies are carried out to investigate their influence on metallic plates. According to [4] which is a study over the influence of projectile geometry on aluminum alloy targets, the blunt projectiles can penetrate more efficiently followed by hemispherical and ogive nosed projectiles, respectively, if the target thickness to projectile diameter ratio is less than one. Another study [5] found that blunt projectiles penetrated the target more efficiently than conical projectiles when the thickness of target was moderate. For the case of thin and thick targets however, an opposite trend was observed.

It is evident from the literature survey that the projectile geometry (nose shapes), impact velocities and target thickness are very important characteristics over the penetration capability [3]. The present work deals with numerical investigation of impact behavior of different geometrical configurations of armor-piercing projectiles.

Different types of methods which permits to evaluate with maximum efficiency the resources needed in different types of products design jobs were developed in the past few years. Some of these methods in the present time are numerical simulations which are a good choice as an instrument for the resource's consumption estimation. These types of methods are encouraged in ammunitions design too.

As an example, we can observe that some military standards encourage the use of numerical simulation in first steps of a product design or on his life cycle, before experimental testing [6].

A number of numerical simulations are conducted to investigate the influences of nose shape and impact velocity over the performance parameters in terms of ballistic limit. Also, the velocity drop, the absorbed energy and the deformation modes are investigated. Finite element simulations of the problem were carried out using finite element code Ansys Explicit Dynamics. Residual velocities of the projectiles were obtained using the post processing module of the code.

II. CAD MODELS

The 3D models of projectiles used for simulation in this study are made in SolidWorks CAD software. As the literature survey suggested, three nose shape geometrical configuration are chosen for this study and they are presented in longitudinal section view as it follows:

- Ogival configuration (Fig. 1);

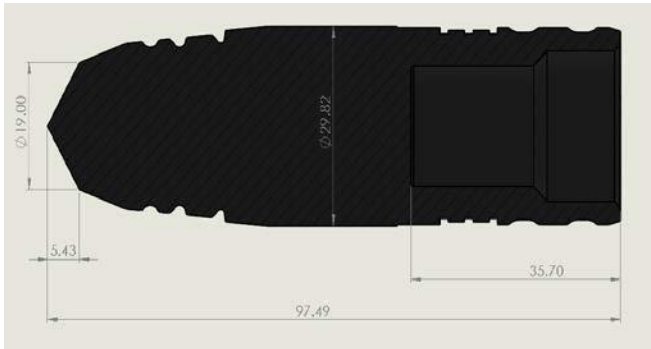


Figure 1. Model for ogival shape configuration for AP-T projectile (section view)

- Blunt configuration (Fig. 2);

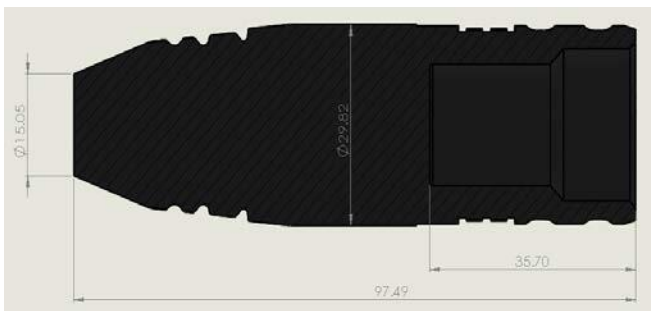


Figure 2. Model for blunt shape configuration for AP-T projectile (section view)

- Hollow point configuration (Figure 3).



Figure 3. Model for hollow point shape configuration for AP-T projectile (section view)

All the three armor-piercing projectiles models are designed in such manner that the only significant difference is the nose shape of each other. The general characteristics for all three forms of projectiles used in simulations are described in Table I.

TABLE I. GENERAL CHARACTERISTICS OF PROJECTILES

Characteristic		Value
Caliber		29.82 mm
Length		97.49 mm
Mass	Ogival	358.50 g
	Blunt	362.30 g
	Hollow Point	357.50 g
Material		AISI S-7 Steel
Initial Velocity		890 m/s

The characteristics of AISI S-7 Steel are presented in Table II.

TABLE II. CHARACTERISTICS OF AISI S-7 STEEL

Characteristic	Value
Material Density	7.76 g/cm ³
Hardness, Rockwell C	61
Tensile Strength, Ultimate	640 MPa
Tensile Strength, Yield	380 MPa
Modulus of Elasticity	207 GPa
Poisons Ratio	0.27-0.30

III. SIMULATIONS SET-UP

The simulations consist in three Explicit Dynamics FEA on which the presented geometrical forms are tested. The main objective of these tests is to study the behavior of projectiles on impact over a 150×150×12 mm AISI 4340 steel plate (Fig. 4) at a velocity of 890 m/s. In order to perform the simulation, simplified forms of projectile are used. (Fig. 5a – Ogival geometry configuration with a simulated mass of 379 g, Fig. 5b – Blunt geometry configuration with a simulated mass of 390 g, Fig. 5c – Hollow point geometry configuration with a simulated mass of 385 g). Also, no ballistic capes were simulated and the angular velocities of the projectiles were neglected.

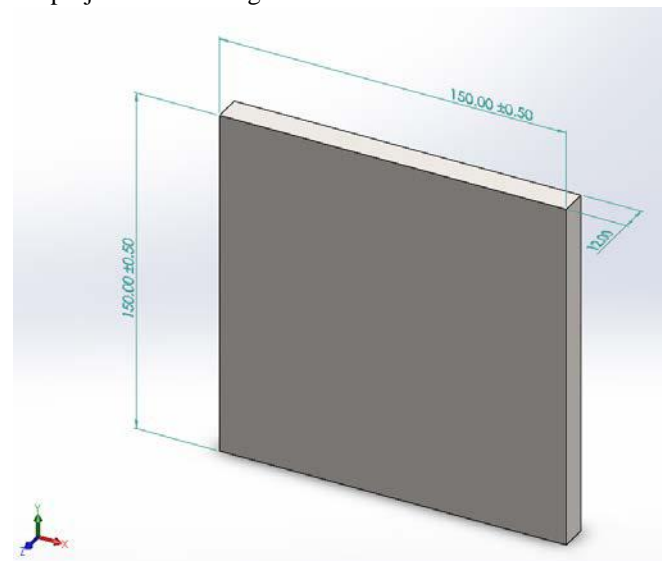


Figure 4. AISI 4340 Steel 150×150×12 mm impact plate

The main characteristics studied in these three simulations are the capability to perforate the impact plate and the

residual velocity of the projectile.

An armor-piercing projectile is considered to be more practical if the residual velocity after the perforation has a great value because it possesses a great amount of kinetic energy which can produce more damages.

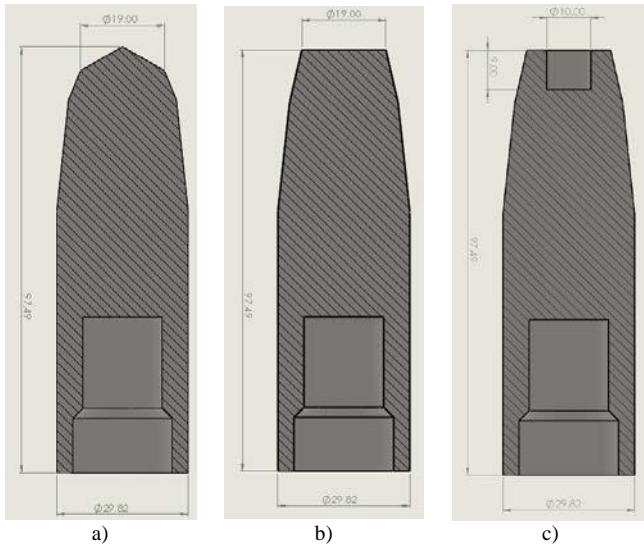


Figure 5. a) Ogival geometry configuration with a simulated mass of 379 g, b) Blunt geometry configuration with a simulated mass of 390 g, c) Hollow point geometry configuration with a simulated mass of 385 g

The characteristics of AISI S-7 steel are presented in Table III.

TABLE III. CHARACTERISTICS OF AISI 4340 STEEL

Characteristic	Value
Density	7.85 g/cm ³
Hardness, Brinell	217
Hardness, Rockwell C	17
Modulus of Elasticity	205 GPa
Tensile Strength, Ultimate	745 MPa
Tensile Strength, Yield	470 MPa
Poisson's ratio	0.28

The simulation assembly for each test consists of one projectile and one S-7 Steel impact plate.

The SolidWorks CAD models (Fig. 6) are imported into ANSYS Explicit Dynamics FEA (Fig. 7) in order to perform the simulation.

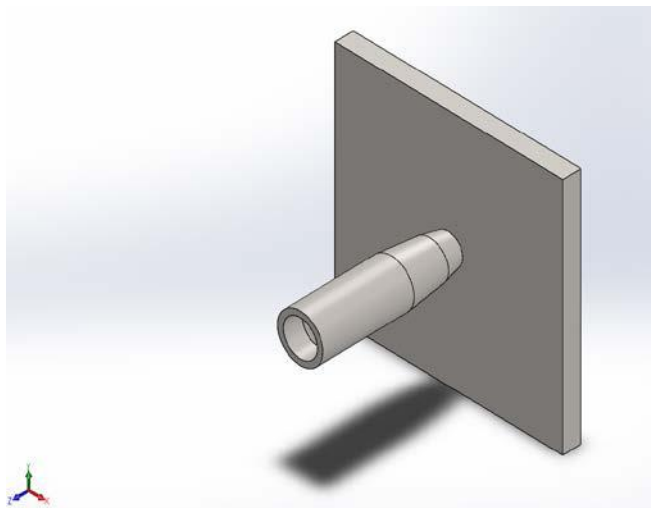


Figure 6. SolidWorks CAD simulation assembly

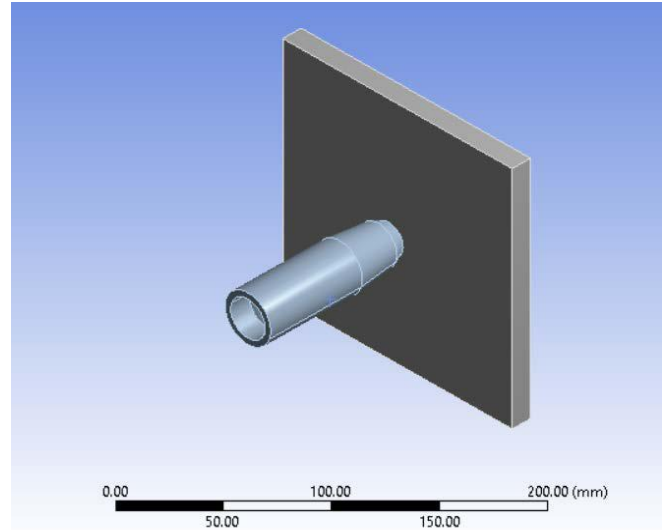


Figure 7. ANSYS Explicit Dynamics FEA simulation assembly

IV. SIMULATIONS

In this chapter are presented the main characteristics of simulations conducted in order to observe the behavior of the projectiles on the impact with a steel plate.

A. FEA simulation of ogival geometrical configuration

The FEA simulation geometry for ogival nose shape projectile study is presented in Figure 8. For this analyze were used one simplified ogival nose shape projectile and one 12 mm thick AISI4340 steel plate.

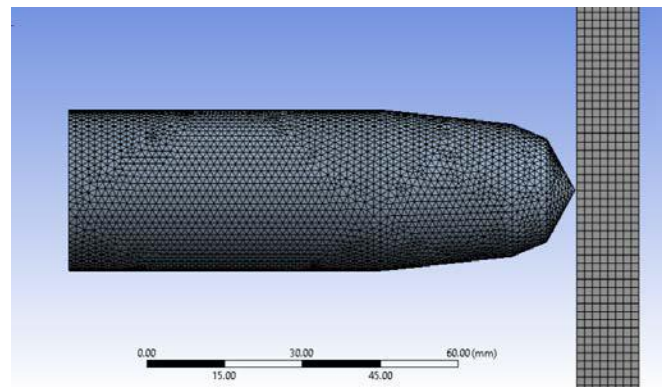


Figure 8. Discretization in finite elements of ogival shape projectile

In Table IV are presented the Simulation settings and characteristics.

TABLE IV. CHARACTERISTICS OF OGIVAL NOSE SHAPE SIMULATION

Characteristic	Value
Initial distance between bodies	0.3 mm
Projectile Material	AISI S-7 Steel
Plate Material	AISI 4340 Steel
Projectile Mesh Element Size	1.4 mm
Steel Plate Mesh Element Size	1.5 mm
Mesh total nodes	114663
Mesh total elements	195787
Initial velocity	890 m/s
End Time of simulation	0.6 ms
Erosion	On Geometric Strain Limit
	Geometric Strain Limit = 0.9
Fixed Support	Two Faces

B. FEA simulation of blunt geometrical configuration

The FEA simulation geometry for blunt nose shape projectile study is presented in Fig. 9. For this analyze were used one blunt nose shape projectile and one 12 mm thick AISI 4340 steel plate.

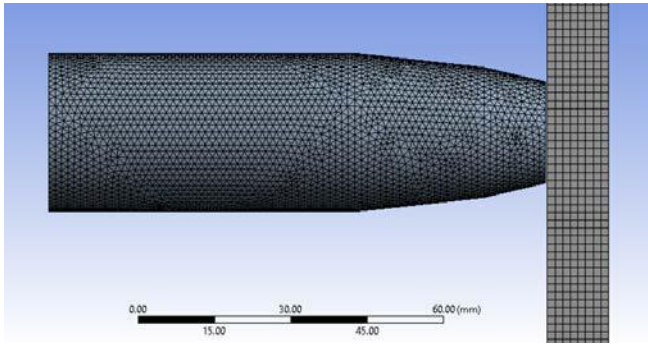


Figure 9. Discretization in finite elements of blunt shape projectile

In Table V are presented the simulation settings and characteristics.

TABLE V. CHARACTERISTICS OF BLUNT NOSE SHAPE SIMULATION

Characteristic	Value
Initial distance between bodies	0.3 mm
Projectile Material	AISI S-7 Steel
Plate Material	AISI 4340 Steel
Projectile Mesh Element Size	1.4 mm
Steel Plate Mesh Element Size	1.5 mm
Mesh total nodes	115133
Mesh total elements	198215
Initial velocity	890 m/s
End Time of simulation	0.6 ms
Erosion	On Geometric Strain Limit
	Geometric Strain Limit = 0.9
Fixed Support	Two Faces

C. FEA simulation of hollow point geometrical configuration

The FEA simulation geometry for hollow point nose shape projectile study is presented in Fig. 10. For this analyze were used one simplified blunt nose shape projectile and one 12 mm thick AISI 4340 steel plate.

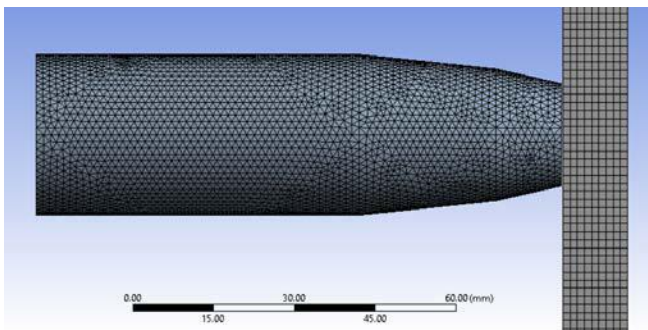


Figure 10. Discretization in finite elements of hollow point shape projectile

In Table VI are presented the simulation settings and characteristics.

TABLE VI. CHARACTERISTICS OF HOLLOW POINT NOSE SHAPE SIMULATION

Characteristic	Value
Initial distance between bodies	0.3 mm
Projectile Material	AISI S-7 Steel

Plate Material	AISI 4340 Steel
Projectile Mesh Element Size	1.4 mm
Steel Plate Mesh Element Size	1.5 mm
Mesh total nodes	125964
Mesh total elements	211372
Initial velocity	890 m/s
End Time of simulation	0.6 ms
Erosion	On Geometric Strain Limit
	Geometric Strain Limit = 0.9
Fixed Support	Two Faces

V. RESULTS

A. Results of ogival geometrical configuration simulation

In Figure 11 is presented the result of simulation. As it can be observed, the plate has been perforated.

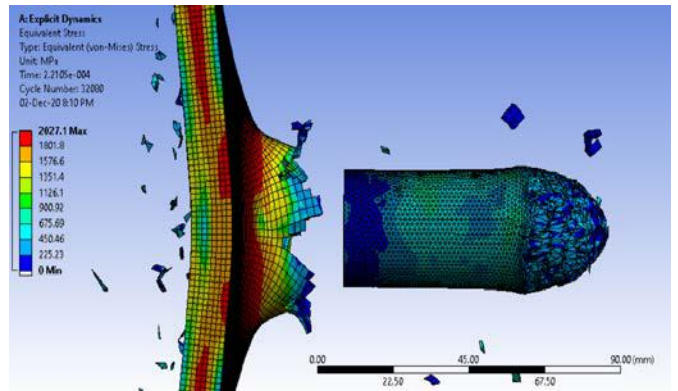


Figure 11. Ogival nose shape FEA simulation results

In Table VII are presented the ogival nose shape FEA simulations results

TABLE VII. CHARACTERISTICS OF OGIVAL NOSE SHAPE SIMULATION

Characteristic	Value
Perforation of the steel plate	Yes
Residual velocity of the projectile	772 m/s
Maximum Equivalent Stress	2027 MPa

Fig. 12 presents the evolution of velocity for the ogival geometry configuration during simulation.

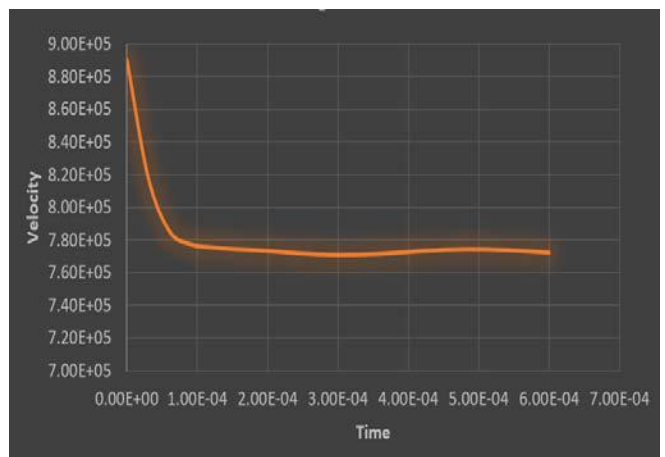


Figure 12. Evolution of velocity for the ogival geometry projectile

B. Results of blunt geometrical configuration simulation

In Fig. 13 is presented the result of simulation. As it can be observed, the plate has been perforated.

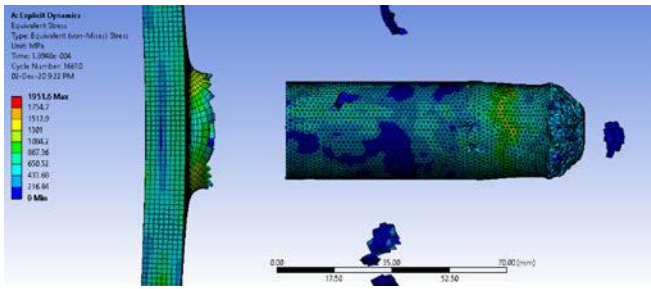


Figure 13. Blunt nose shape FEA simulation results

In Table VIII are presented the blunt nose shape FEA simulations results

TABLE VIII. CHARACTERISTICS OF BLUNT NOSE SHAPE SIMULATION

Characteristic	Value
Perforation of the steel plate	Yes
Residual velocity of the projectile	768 m/s
Maximum Equivalent Stress	1951.6 MPa

Fig. 14 presents the evolution of velocity for the blunt geometry configuration during simulation.

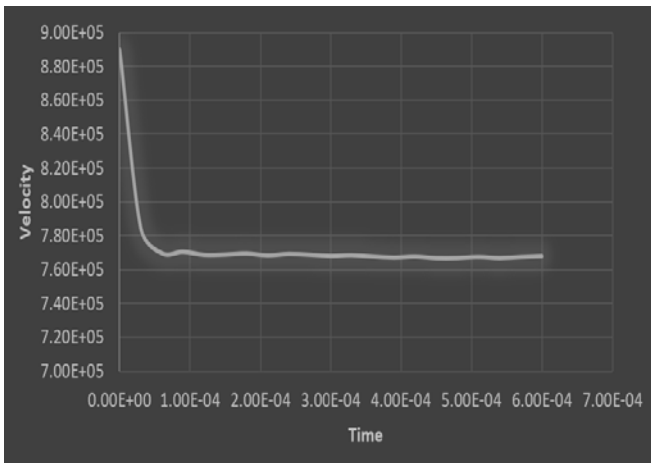


Figure 14. Evolution of velocity for the blunt geometry projectile

C. Results of hollow point geometrical configuration simulation

In Fig. 15 is presented the result of simulation. As it can be observed, the plate has been perforated.

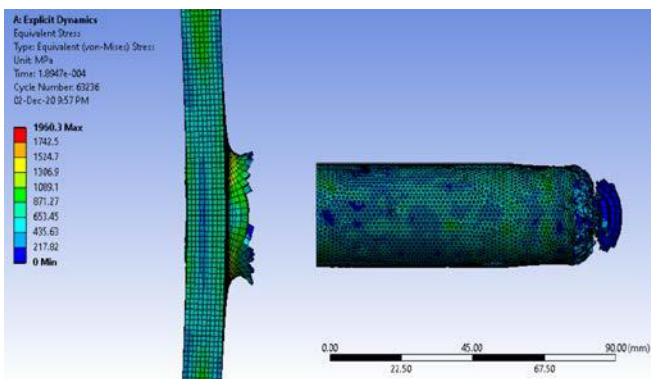


Figure 15. Hollow point nose shape FEA simulation results

In Table IX are presented the ogival nose shape FEA simulations results

TABLE IX. CHARACTERISTICS OF HOLLOW POINT NOSE SHAPE SIMULATION

Characteristic	Value
Perforation of the steel plate	Yes
Residual velocity of the projectile	755m/s
Maximum Equivalent Stress	1960 MPa

Fig. 16 presents the evolution of velocity for the hollow point geometry configuration during simulation.

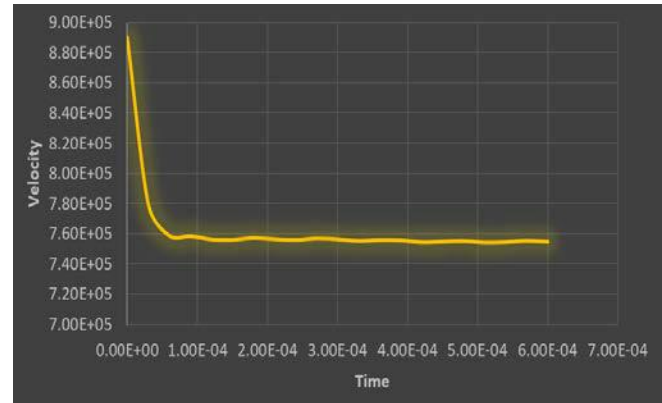


Figure 16. Evolution of velocity for the hollow point geometry projectile

VI. CONCLUSION

After analyzing the data obtained from the simulations, it is pointed out that at a velocity of 890 m/s the 30 mm proposed projectiles can easily perforate a 12 mm steel plate. The obtained results are presented in Table X.

TABLE X. OBTAINED RESULTS OF THE SIMULATIONS

Characteristic	Ogival geometry	Blunt geometry	Hollow Point geometry
Perforation of the steel plate	Yes	Yes	Yes
Mass of the simulated projectile	379 g	390 g	385 g
Initial velocity	890 m/s	890 m/s	890 m/s
Residual velocity of the projectile	772 m/s	768 m/s	755 m/s
Drop of the projectile velocity	13.26%	13.71%	15.16%
Initial Kinetic Energy of the projectile	150.1 kJ	154.46 kJ	152.48 kJ
Residual Kinetic Energy of the projectile	112.94 kJ	115.02 kJ	109.73 kJ
Drop of the projectile's Kinetic Energy	24.75%	25.53%	28.04%
Maximum Equivalent Stress	2027 MPa	1951.6 MPa	1960 MPa

Fig. 17 presents the evolution of velocities for the studied projectiles during simulations.

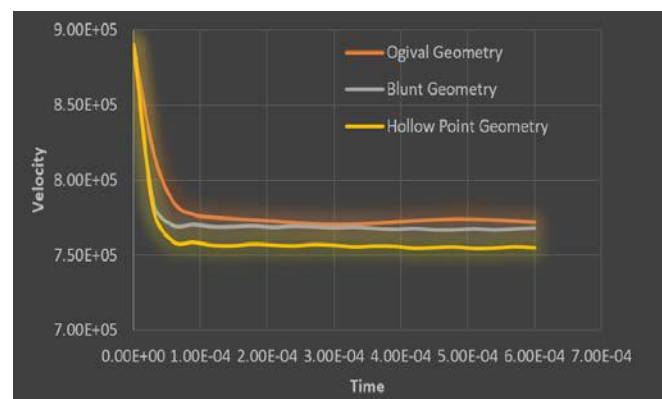


Figure 17. Evolution of velocities for the studied projectiles

The response of AISI 4340 12 mm plate subjected to normal impact by Ogival, Blunt and Hollow Point projectiles in the velocity range of 890 m/s has been analyzed using numerical simulations using ANSYS Explicit Dynamics FEA. The present analysis can be used as a benchmark for designing armor-piercing projectiles and also for protective equipment's components subjected to impact loading. Based on the detailed investigations the following conclusions can be drawn:

- All three AP projectile configurations studied were able to perforate into the armor due to their high kinetic energy. The perforation power is dependent on the mechanical characteristics of the armor, the shape and the resistance of the projectiles and the remaining energy of each projectile configuration at the impact with the armor plate.
- The residual kinetic energy of all three types of tested projectiles drops rapidly after the perforation, but the residual kinetic energy is still enough to produce more damages.
- The geometrical configurations tested in this study have similar results in similar conditions, as it can be seen in Table X, but the ogival geometrical configuration performs better than the other two configurations

considered in this study based on the registered values of the residual speed and of the kinetic energy.

REFERENCES

- [1] H. Seton-Karr, "Ammunition," in *Encyclopedia Britannica*, H. Chisholm, UK, Cambridge University Press, 1911, 11th Ed., pp. 864–875.
- [2] "Construction, Operation, Effects and Calculation of Ammunition - Artillery Engineer Course, Part I", Military Academy Printing House, Bucharest, 1980 (in Romanian).
- [3] A. Husain, R. Ansari, and A. Khan, "Experimental and Numerical Investigation of Perforation of Thin Polycarbonate Plate by Projectiles of Different Nose Shape," *Latin American Journal of Solids and Structures*, Feb. 2017, <https://doi.org/10.1590/1679-78253252>.
- [4] A. L. Wingrove, "The influence of projectile geometry on adiabatic shear and target failure," *Metallurgical Transactions A* 4, 1973, pp. 1829-1833.
- [5] T. W. Ipson and R. F. Recht, "Ballistic Perforation by Fragments of Arbitrary Shape," Denver Research Institute, Naval Weapons Centre, China Lake, CA, NWC TP 5927, 1977.
- [6] G. Surdu and G. Slămnoiu, "Considerations on Efficiency in Experimental Tests Specific for Projectiles of Low Caliber," *Procedia Economics and Finance*, vol. 32, pp. 899-905, 2015, doi:10.1016/S2212-5671(15)01541-5.
- [7] A. C. Sava, Gh. Bărsan, I. Vedinaș, and L. Piticari, "The impact of kinetic projectiles of 76 mm cal. ahead type artillery ammunition on the lifting surface of the aerospace vehicles," *Review of the Land Force Academy*, vol. 21, no. 1, pp. 92-98, 2016.